Do flame describing functions suitably represent combustion dynamics under self-sustained oscillations?

Preethi Rajendram Soundararajan, Guillaume Vignat, Daniel Durox, Antoine Renaud, Sébastien Candel

Do flame describing functions suitably represent combustion dynamics under self-sustained oscillations?

Preethi Rajendram Soundararajan[1], Guillaume Vignat[2], Daniel Durox[3], Antoine Renaud[4], Sébastien Candel[5]

Laboratoire EM2C, CNRS, CentraleSupélec, Université Paris-Saclay, 3 rue Joliot Curie, 91190 Gif-sur-Yvette, France

Abstract

Transfer function concepts that appear in many areas and most notably in control systems have been extensively used to represent the flame response in low-order models of combustion instability. Much of the theoretical work is based on flame transfer functions (FTF). In recent years, its nonlinear extension, namely the flame describing function (FDF), has been used to get a more accurate representation of the flame response when the level of oscillation becomes large and the system reaches a limit cycle. Despite their wide and reasonably successful use in predicting instabilities, the direct validity of using FTF/FDFs to represent the flame response still remains to be experimentally substantiated. This article is aimed at providing a direct assessment of the capacity of the FDF to suitably describe the flame behavior under self-sustained oscillations (SSOs) for a spray-swirl flame anchored by an injector that is weakly-transparent to acoustic waves. This is accomplished by making use of an experimental combustion configuration that not only exhibits unstable oscillations but also features a set of driver units to modulate the flame (namely stable flame modulation or SFM). The flame is modulated at the frequency of SSO, and the amplitude of incident velocity modulations is then progressively varied until it coincides with that found under SSO. The injector dynamics is shown to be different between SSO and SFM for an injector that is weakly-transparent to acoustic waves and imposes a certain degree of decoupling between plenum and chamber. For such injectors, the FDF built with the upstream velocity would not suitably represent SSO, as this lumps the injector and flame dynamics together. It is then important to use velocity measurement at the injector outlet, at a point where the relative velocity fluctuation matches the relative volumetric flow rate fluctuation. The describing function with velocity reference at the injector outlet is measured for various input levels and found to approximately match those measured under SSO. The best match is obtained when the amplitude of external modulation induces a level of velocity oscillations that comes closest to that prevailing under SSO. This demonstrates that the FDF may suitably capture the nonlinearity of the flame response, at least in the configuration investigated in this research.

Keywords: Combustion dynamics, flame transfer/describing function, limit cycle oscillations, injector dynamics, acoustically weakly-transparent injectors.

[1]Corresponding author: preethi.rajendram-soundararajan@centralesupelec.fr

[2]guillaume.vignat@gmail.com. Present address: Stanford University, Department of Mechanical Engineering, Stanford, CA 94305, USA.

[3]daniel.durox@centralesupelec.fr

[4]antoine.renaud@centralesupelec.fr

[5]sebastien.candel@centralesupelec.fr

1. Introduction

This article is dedicated to the memory of Professor J.E. Ffowcs Williams (also known to many of his colleagues and friends as Shôn). Shôn was an influential and brilliant scientist. He contributed quite extensively to aeroacoustics, the science of noise generated aerodynamically. He was also one of the early proponents of anti-sound, the reduction of sound by cancelation with secondary sources of sound. Of course, there were discussions and even experimental demonstrations of this concept, but Ffowcs Williams understood that active noise control could become a reality by making use of advances in adaptive beamforming and optimal control [1]. Ffowcs Williams also considered that similar concepts could be used to control unstable flows, and the principles of sound cancellation implemented in noise control technology could be extended in that direction [2]. He worked out some speculative examples like those of controlling the Kelvin-Helmholtz instability of shear layers or the gravitational instability of stratified fluids [3] and also investigated more practical possibilities like that of suppressing rotating stall and surge instabilities in compressors [2]. Ffowcs Williams cited the progress made in the control of combustion instabilities demonstrated in simple devices exhibiting a single mode of instability and later on in the suppression of acoustically coupled instability in larger-scale experiments on reheat "buzz"[4]. Work in this direction was notably pursued by one of his students, and later colleague, Ann Dowling [5, 6] and her own doctoral students. After many early experiments in active control of combustion, it became clear that progress could only be made by developing modeling methods [7–11], and this gave rise to a considerable research effort that was aimed at representing the combustion system and controller in the framework of control systems theory. The central idea was to describe the combustion response in terms of transfer functions, use closed-loop representations of the coupling that was achieved by acoustic modes and controller actions. Much effort has been devoted to deriving models that could guide the analysis of combustion dynamics phenomena and may then be used as predictive tools. This modeling effort was begun to gain some understanding of the processes leading to unstable oscillations in rocket engine [12–18]. More recently, attention has been focused on dynamical phenomena in gas turbine combustors operating in the premixed mode and using swirling flows to anchor the flames at a distance from the injection units [9, 19–29]. The present article addresses a central modeling issue in the context of swirl stabilized flames. Is it possible to suitably describe the combustion response in terms of transfer functions or their nonlinear extension, describing functions? In other words, can one model a complex multi-dimensional flow characterized by the presence of multiple scales, those of turbulence and combustion, and the fast kinetics of strongly exothermic reactions in terms of low-order dynamical tools relying on transfer or describing functions? Do these reduced descriptions capture the three-dimensional flame dynamics that are involved in the process? This analysis aims at providing a direct experimental proof that transfer functions and their describing functions extensions represent the flame behavior and that the reduced-order model suitably describes the multi-dimensional reality. It is not our intention to give a general answer to the questions raised previously, and the analysis is restricted to a case that has much practical importance, that of swirling flames that are compact with respect to the acoustic wavelength of the coupling modes. This case will be investigated experimentally to highlight the difficulties and limitations of this kind of representation and provide some insight on issues of low-order modeling of combustion instabilities.

At this point, it is worth briefly reviewing the state of art in low-order modeling to place the present investigation in perspective. The early analysis of combustion instability relied on the sensitive time lag (STL) theory. The flame response was represented in terms of an interaction index n and a time lag τ that was assumed to be a function of the state variables in the combustion region [12, 14, 15]. In general, these two terms were considered to be parameters that could be varied to determine regions of instability. This kind of model assumed, in essence, that a transfer function existed between the state variable disturbances and combustion disturbances such as those of the heat release rate. The gain of this transfer function was a constant proportional to the interaction index n, while the phase was a linear function of the angular frequency $\varphi_F = \omega\tau$. More recently, considerable effort was expended to understand mechanisms controlling instabilities and to represent the flame dynamics in terms of transfer functions. This effort is reviewed, for example, in [9, 26, 30, 31]. The transfer function was introduced to link relative fluctuations of heat release rate in the flame, treated as an output, to the relative fluctuations in volume flow rate. When the relative velocity fluctuation and the mean velocity at the input are uniform, it is possible to consider

that the relative volume flow rate fluctuation is equal to the relative velocity fluctuation. For experimental convenience, velocity fluctuation is then considered as the input instead of volume flow rate fluctuation. The transfer function may have multiple inputs, and in the present case, one other input could be the perturbations in equivalence ratio. For the case considered in this article, the mode of combustion is quasi-premixed, and the primary input is the disturbance in velocity (representing the disturbance in volume flow rate). The transfer function is given by

$$\mathcal{F}_0(\omega) = \frac{\dot{Q}'(\omega)/\overline{\dot{Q}}}{u'/\overline{u}} = G_F(\omega)\mathrm{e}^{\mathrm{i}\varphi_F(\omega)} \tag{1}$$

Transfer functions were introduced, in particular, to derive active control methods and help interpret their experimental demonstrations. Transfer function expressions were obtained for many simple flames like premixed conical and "V" flames and for swirling premixed flames [32–42] and were compared in some cases with experimental data. It was then recognized that the flame response depended not only on frequency but also on the amplitude of oscillation. This led to the replacement of the FTF by a describing function, i.e., a family of transfer functions with each of these functions depending on the amplitude of the input.

$$\mathcal{F}(\omega, u') = \frac{\dot{Q}'(\omega, u')/\overline{\dot{Q}}}{u'/\overline{u}} = G_F(\omega, u')\mathrm{e}^{\mathrm{i}\varphi_F(\omega,u')} \tag{2}$$

This was employed, for example, in a theoretical analysis of the dynamics of a ducted flame by Dowling [43], which indicated only a gain saturation with the velocity fluctuation amplitude. The concept of flame describing function (FDF) was generalized by Noiray et al. [44] to also consider phase dependence with respect to the amplitude of perturbations. The FDF was shown to provide an understanding of many non-linear features observed experimentally, like frequency shifting during oscillation growth, mode switching (frequency jumping during oscillation), instability triggering, and hysteresis, and more generally represent the dynamics of finite amplitude oscillations [45]. This has been a notable advance because the describing function allowed to retrieve nonlinear dynamical features [46–59]. Models using the FDF yield amplitude-dependent results that allow direct comparisons with experimental data since most instability experiments are carried out when the oscillations are established and have reached a finite value. It was, however, found that the FDF has limitations and cannot easily handle situations where the limit cycle amplitude evolves as a function of time and the amplitude becomes irregular giving rise to "galloping" limit cycles (GLCs), or modulated in a more regular fashion when the oscillation is sustained by two modes. These cases require extensions of the FDF in the form of multiple-input describing functions [58, 60, 61]. A practical difficulty encountered while obtaining the FDF is the need for measuring the heat release rate fluctuations $\dot{Q}/\overline{\dot{Q}}$ from the flame. This is often deduced from the fluctuations of light intensity originating from excited radicals such as OH^* or CH^* present in the reaction zone and considering that these intensities are monotonically related to the heat release rate fluctuations. This is well validated for fully premixed flames [62], but might not be fully applicable to the case of non-premixed or technically premixed systems. In such cases and in configurations where optical access to the flame is not available, an alternative purely acoustic method consists in determining the flame transfer matrix (FTM) [23, 63]. In this framework, the flame is represented by a 2×2 transfer matrix $\boldsymbol{T}$, and the acoustic states upstream and downstream of the flame are obtained using multiple microphones. This method has been widely adopted for modeling industrial gas turbines which do not have optical access to the flame. It is also useful for technically premixed flames where the quantitative estimate of heat release rate using chemiluminescence is not well validated. However, being a purely acoustic method, FTM does not account for the convective disturbances that result from interactions between acoustic waves and flow singularities, like those associated with swirlers and injection units [64]. In practice, the method yields a transfer matrix $\boldsymbol{T}$ corresponding to the combination of a flame transfer matrix $\boldsymbol{F}$ and injector transfer matrix $\boldsymbol{B}$, and the flame transfer matrix is deduced from $\boldsymbol{F} = \boldsymbol{T}\boldsymbol{B}^{-1}$. It requires a separate measurement of the injector matrix $\boldsymbol{B}$ obtained under cold flow conditions and the inversion of this matrix. One assumes that $\boldsymbol{B}$ does not change under hot fire conditions. Uncertainties also arise from practical application in a highly noisy background in which the coherence between the forcing and microphone signals may not be very high. The FTM is also experimentally complex as it requires measurements

at two independent acoustic states of the system which imply modulation and signal acquisition on the upstream and downstream sides of the injector unit. Independent acoustic states of the system can also be achieved either by increasing the combustion chamber length or changing the impedance at the outlet. While former has the disadvantage of triggering self-sustained modes, the latter can be difficult to achieve. These techniques are not always feasible, and in such cases, one may prefer direct FDF measurements.

Whatever the framework (FDF or FTM), it is worth asking whether the low-order models in which the flame response is treated as a black box can suitably represent the fluid and combustion dynamics that determine thermoacoustic instabilities. Although many previous studies in the literature (including [44] and more recently [65]) have demonstrated the capability of FDFs in instability prediction, thus constituting an indirect validation of the methodology, no direct experimental proof is available to verify if the FDF suitably renders the combustion dynamics under self-sustained oscillations (SSO). This question is represented schematically in Fig. 1(a) and (b).

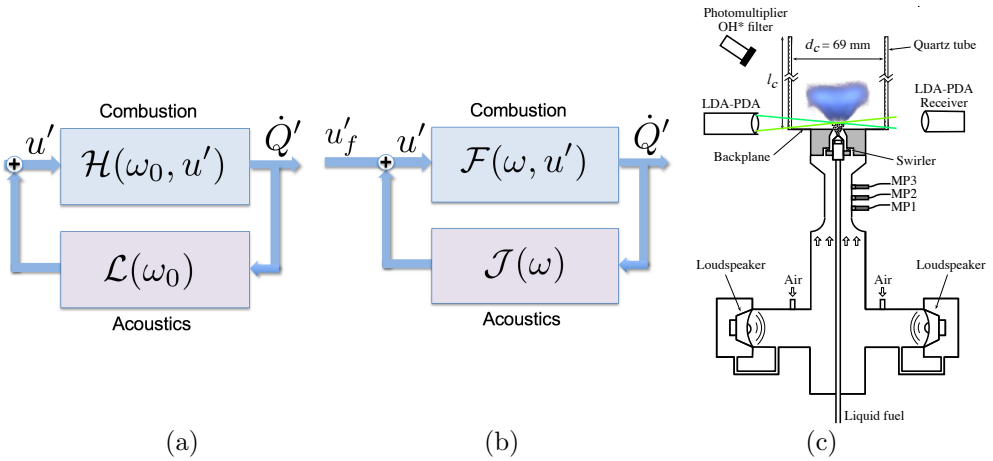

Figure 1: (a) Closed-loop representation of a self-sustained instability at an angular frequency ω_0 and an amplitude of oscillation u'. The function $\mathcal{H}$ represents the flame response in the self-sustained oscillation. (b) Stable flame operation obtained by changing the acoustic coupling. This is used to allow external modulation and the determination of the flame describing function $\mathcal{F}(\omega, u')$ by imposing $u'_f = v_0 e^{-i\omega t}$. (c) Schematic of the experimental setup SICCA-Spray.

This figure shows on the left a representation of the system when it is executing self-sustained oscillations (SSO) and features a limit cycle at an angular frequency ω_0. The flame dynamical response is $\mathcal{H}(\omega_0, u')$. The inclusion of u' in this expression is to indicate that the flame behavior is also controlled by the level of incident disturbances. In the center, the diagram shows the combustor operating in a stable manner and being modulated externally to measure the FDF designated as $\mathcal{F}(\omega, u')$. Of course, this cannot be done if the system features a self-sustained oscillation. The harmonic modulation can be applied when the flame is stable. It was pointed out by a reviewer that one cannot separate the flame from its environment so that an acoustic coupling is always present. However, this coupling may be reduced by shifting the roots of the dispersion relation that give rise to unstable oscillations. The method is explained with a model problem treated in Appendix A. It is shown there that the flame may be made to operate in a stable regime by changing the acoustic feedback. This is represented in Fig. 1 by replacing $\mathcal{L}$ with $\mathcal{J}$ and achieved in practice by changing the combustion chamber size to remove the resonant frequencies out of the range of interest manifested under SSO. One may then see if $\mathcal{F}$ and $\mathcal{H}$ coincide or, more precisely if

$$\mathcal{F}(\omega_0, u') \simeq \mathcal{H}(\omega_0, u') \tag{3}$$

It is worth underlining that the flame dynamics under SSO represented by $\mathcal{H}$ cannot be a priori considered to coincide with the FDF $\mathcal{F}$ determined under stable flame modulation (SFM) because (1) these descriptions are only a reduced model of reality, and (2) the FDF is determined in an environment that differs from the

one considered under SSO. A good match between these two functions will indicate that a low-order model using a measured FDF may suitably represent the real system and will provide reasonable predictions of SSO. However, one cannot be certain that the flame behavior has not been modified when the loop is closed and when a strong acoustic coupling takes place. A modification of this type is not considered in control systems where the transfer function or describing function of the "plant" does not depend on the feedback path. Here the situation is different because the flame is a result of a complex multidimensional flow where exothermic reactions take place, and one cannot be certain that the low-order modeling based on the FDF suitably represents the flame dynamics under SSO.

This article begins with a presentation of the experimental setup (section 2). Flame dynamics are then examined using OH^* chemiluminescence images in section 3 under SSO and compared to those corresponding to external modulation (referred to as stable flame modulation or SFM). A comparison between the flame response $\mathcal{H}$ and the FDF $\mathcal{F}$ is then carried out in section 4. This is followed by section 5, which is focused on the injector dynamics under SSO and SFM. It is shown in that section that the injector operates in a different manner when the system is modulated from upstream and when the system executes self-sustained oscillations. This has consequences in terms of low-order modeling that are also briefly examined.

2. Experimental set-up

Experiments are carried out in a generic single injector setup (SICCA-Spray). This configuration, shown schematically in Fig. 1(c), comprises a plenum, a swirl-spray injector, and a cylindrical chamber. Liquid heptane fuel is delivered as a hollow cone spray by a simplex atomizer producing a dispersion of fine fuel droplets. The atomizer is recessed at a distance of 6.75 mm with respect to the combustor backplane. The mass flow rate of fuel is set by a Bronkhorst CORI-FLOW controller with a relative accuracy of 0.2%. The air flow rate measured by a Bronkhorst EL-FLOW mass flow controller with a relative accuracy of 0.6% is injected at the bottom of the plenum. The stream of air enters the chamber through an injection unit described in detail in a recent publication [66]. This unit comprises an air distributor leading to a tangential swirler with six channels. This element induces a clockwise rotation of the flow. The air and the fuel spray are delivered to the combustor through a conical section having an 8 mm diameter outlet. A swirler, designated as 716, is used in the present investigation. The swirl number, determined experimentally by integrating the velocity profiles at the outlet of the injector at a height of 2.5 mm above the backplane, is $S_N = 0.70$ (refer to [66] for swirler characteristics). The burner is operated at a global equivalence ratio of $\phi = 0.95$, which corresponds to an air flow rate of $2.3\,\mathrm{g\,s^{-1}}$ and a fuel flow rate of $520\,\mathrm{g\,h^{-1}}$. The combustion chamber is formed by a fully transparent cylindrical quartz tube providing complete optical access to the combustion zone. Self-sustained oscillations of the system are obtained by varying the chamber length l_c. One finds in this way different resonant frequencies and amplitudes of longitudinal limit cycle instabilities. During the measurement of FDFs under SFM, a chamber length of $l_c = 150$ mm is chosen to operate the system under stable conditions. For these measurements, two driver units located at the bottom of SICCA-Spray are excited to achieve different levels of fluctuations. These driver units are modulated at the same frequencies as those of SSO and at an amplifier voltage that is close to the level of relative fluctuations observed under SSO. When the system is operating under SSO, the driver units are left inactive.

2.1. Diagnostics

The SICCA-Spray experimental setup comprises three microphones plugged on the plenum, designated as MP1, MP2, and MP3 in Fig. 1(c). These sensors are Brüel & Kjær 4938 microphones mounted with type 2670 preamplifiers having a relative accuracy of 1% and a passband frequency set between 15 Hz and 20 kHz. Apart from the measurement of pressure signals, these microphones are also used to determine the acoustic velocity fluctuations with the multi-microphone method [67]. Velocity fluctuations in the chamber are measured with a Dantec two-component phase Doppler anemometer (PDA). This measurement is directly obtained on the spray of heptane droplets. To have the best attainable data rate, the measurements are performed with the system configured exclusively for anemometric measurements (laser Doppler anemometry, LDA), which

allows only for the evaluation of axial velocity from heptane droplets. Details on the velocity measurement location is given in section 2.2. The transmitting optics of the system produces a 532 nm laser beam that is split into two parallel beams. One of the beams is shifted in frequency after passage through a Bragg cell. The focal length of the transmitting optics is 500 mm and that of the receiving optics is 310 mm. The theoretical size of the laser beam intersection as viewed by the receiving optics is $0.14 \times 0.14 \times 0.23$ mm.

An estimate of heat release rate (HRR) integrated over the flame volume is obtained by measuring the OH^* chemiluminescence (with a 10 nm filter centered at 308 nm) from the flame using a photomultiplier tube. The validity of using OH^* chemiluminescence as a HRR indicator has been systematically validated in the current configuration in [65]. The spray flame considered in this study is found to operate in a quasi-premixed fashion due to the recessed position of the atomizer inside the injector. This positioning allows a part of the fuel spray to impinge on the conical section of the injector nozzle, which fluctuates along with the air flow. The equivalence ratio fluctuations, therefore, remain low at the injector outlet compared to the velocity fluctuations, and there is no significant spatial stratification in the flame zone. The readers are referred to [65] for the detailed analysis. Additionally, a PI-MAX intensified CCD camera from Princeton Instruments is used to obtain the flame images. The signals from the plenum microphones and photomultiplier are sampled simultaneously during the velocity measurements by the LDA system for a period of 10 s and at a data rate of roughly 25,000 Hz.

2.2. Velocity measurement location

The velocity measurement for the determination of FDF (defined by Eq. 2) is obtained at the injector outlet using LDA. When using a swirling injector, the velocity profile at the exit of the injector is nonuniform, and this raises a question on choosing an optimal position for the measurement. Normally FDFs are defined, in the absence of equivalence ratio fluctuations, as the ratio of relative heat release fluctuations to the relative volumetric flow fluctuations ($\dot{q}'_v/\bar{\dot{q}}_v$). However, from a practical viewpoint, it is difficult to measure relative volumetric flow rate fluctuation, and this quantity is generally replaced by the relative velocity fluctuation as in Eq. (2). This defines a condition for determining the reference position for velocity measurements; one must choose a location at the exit of the injector where the relative velocity fluctuation coincides with the relative volumetric flow rate fluctuation. The measurements and the subsequent determination of this location are detailed in [65]. For the swirler 716, the reference position for the measurement of velocity is located at a distance of $r = 4$ mm from the center of the injector and at a height of $h = 2.5$ mm from the backplane. The measured axial velocity at the exit of the injector is henceforth referred to as $u_{c,r}$. At the reference position, the mean droplet size of heptane spray is 4.5 µm, and hence it can be reasonably assumed that the droplet velocity at this point is equivalent to the flow velocity.

3. Flame dynamics

Before examining the FDF and the flame response in terms of a gain and phase, it is logical to compare the flame dynamics under SSO and SFM using OH^* chemiluminescence images as presented in Fig. 2. The images are captured by a PI-MAX intensified camera equipped with a Nikon 105 mm UV lens and an Asahi optical bandpass filter (10nm centered at 310 nm corresponding to emission bands of OH* radicals in the flame). The camera is triggered with respect to the instability using the photomultiplier signal, which is low pass filtered with a cut-off frequency of 800 Hz using an analog filter. This improves triggering by reducing the jitter present in the photomultiplier signal. A Tektronix TBS 2000 oscilloscope provides a trigger signal when the filtered photomultiplier signal reaches its mean value and at its rising edge. This setup is used to obtain the phase averaged flame images shown in Fig. 2. The exposure is 40 µs long. The images appearing in Fig. 2 are averaged over 1000 individual samples and processed with an Abel inversion algorithm.

For the measurements, the quartz tube for the unstable case is 265 mm long and the limit cycle features a frequency of 533 Hz. The amplitude of velocity oscillation at $(r, z) = (4.0, 2.5)$ mm measured using LDA is $u'_{c,r}/\overline{u}_{c,r} = 9\%$, and that of the chemiluminescence signal is $I'_{OH^*}/\overline{I_{OH^*}} = 28.9\%$. Here and henceforth, the notation $(\cdot)'$ refers to the root mean square (RMS) fluctuations, and $\overline{(\cdot)}$ refers to the mean of a quantity. The flame dynamics under SSO is shown in Fig. 2(a) and stable flame modulation is examined in Fig. 2(b-d). In

Fig. 2(b), directly underneath the SSO images, the forcing level is set to match the conditions encountered under SSO. In Fig. 2(c), the forcing level is significantly lower, while in Fig. 2(d), it is significantly higher.

Figure 2: (a-d) Phase-averaged, Abel-transformed flame images shown in false colors. Light intensity of OH* chemiluminescence is obtained at different phase instants of the acoustic cycle using an intensified camera. (a) Images obtained under SSO at a frequency $f_0 = 533$ Hz. $I'_{OH^*}/\overline{I_{OH^*}} = 28.9\%$. (b-d) Images corresponding to SFM at the frequency of SSO. (b) The forcing amplitude matches that observed during SSO ($I'_{OH^*}/\overline{I_{OH^*}} = 30.4\%$). (c) The forcing amplitude is lower than that observed during SSO ($I'_{OH^*}/\overline{I_{OH^*}} = 14.2\%$). (d) The forcing amplitude exceeds that observed during SSO ($I'_{OH^*}/\overline{I_{OH^*}} = 37.8\%$). (e-g) Flame isocontours determined by Otsu thresholding method for SSO (solid line in (e-g)) and three levels of SFM (same—dotted line in (e), lower—dotted line in (f), and higher—dotted line in (g) fluctuation level compared to SSO).

The set of images in (a) and (b) indicate that the flame shapes and intensity corresponding to SSO agree with those of SFM at 3.5 V, i.e., when the velocity fluctuation levels match. On comparing SSO with SFM at other amplifier voltages where the velocity fluctuations do not match, some minor differences can be observed in the flame shapes and intensity levels. A periodic elongation and widening is visible in all the cases starting from $\Phi = 3\pi/2$ and extending till $\pi/2$, the latter corresponding to the broadest flame during the

cycle. To further understand the similarities and differences between SSO and SFM, the flame front location is identified by applying the so-called Otsu thresholding method to the OH^* images, as demonstrated by [68], and is shown in Fig. 2(e-g) when the flame is under SSO (in solid line) and for the four cases of SFM (in dotted line): same, lower, and higher relative intensity fluctuation compared to SSO. The extracted flame contour data evidently show a close match between the SSO and SFM flame shapes when the forcing level of SFM (i.e., at $V_0 = 3.5\,\mathrm{V}$) matches the oscillation level of SSO. At the other two SFM levels, visible differences can be observed in the flame contour shape at certain parts of the cycle. For instance, this difference is more pronounced for the higher fluctuation level between the phase instants $\Phi = \pi/4$ and $3\pi/4$. For the remaining part of the cycle, the difference is minor, with only some observable deviation close to the base of the flame. The difference in the flame contour position between SSO and SFM is more prominent for the lower amplitude case at all the phase instants, except at $\Phi = 7\pi/4$, where the contours corresponding to all four cases nearly collapse.

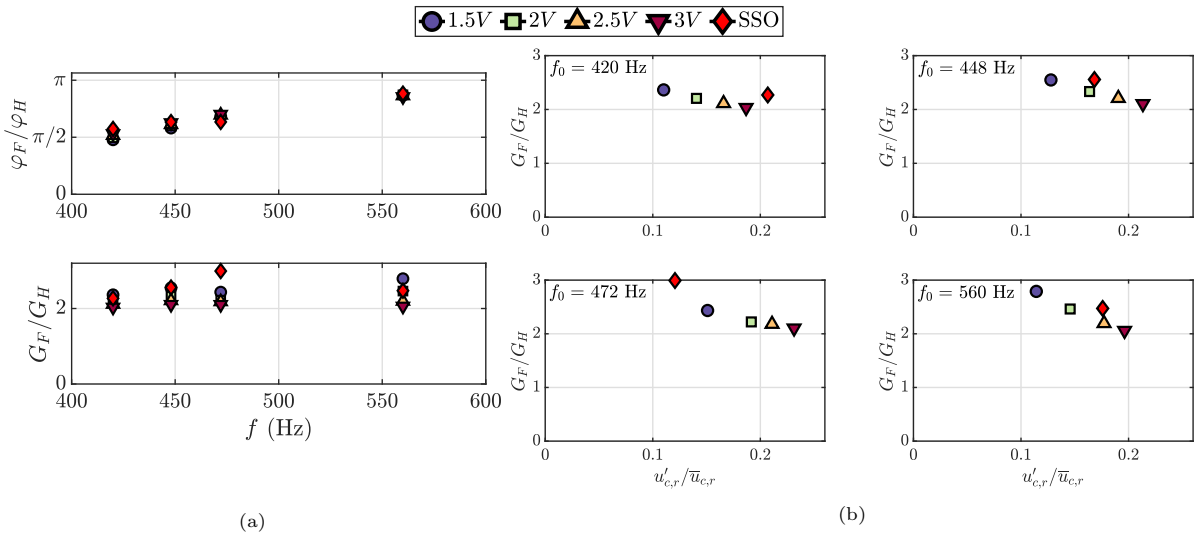

Figure 3: Comparison between the stable flame describing function $\mathcal{F}$ and the combustion response under SSO, $\mathcal{H}$. (a) Phases φ_F and φ_H and gains G_F and G_H plotted at the four resonance frequencies and at different amplitude levels for SFM. The relative velocity fluctuation for obtaining $\mathcal{F}$ and $\mathcal{H}$ is measured in the chamber. The diamond symbols represent phases and gains of $\mathcal{H}$ during SSOs for different chamber lengths. The other symbols correspond to the measured $\mathcal{F}$ during SFM obtained while modulating the flame at the SSO frequencies and at four different levels of amplifier voltages (1.5, 2, 2.5, and 3 V). (b) Gain of $\mathcal{F}$ and modulus of $\mathcal{H}$ plotted as a function of the relative velocity fluctuation in the chamber. The velocity is measured at the reference position $(r, z) = (4.0, 2.5)$ mm. The representation in terms of amplifier voltages shown in (a) is expressed in terms of velocity fluctuation levels in (b).

4. Comparison of FDF and flame response under limit cycle oscillations

The comparison between FDF $\mathcal{F}$ and the flame response $\mathcal{H}$ is shown in Fig. 3(a) in terms of gain and phase at different frequencies. For the measurements under SSO, the chamber length l_c is varied to obtain self-sustained oscillations at different frequencies. Chamber lengths of 250, 300, 315, and 350 mm are used to attain the oscillations at frequencies 560, 472, 448, and 420 Hz, respectively. The measurement under SFM is performed by modulating the flame using the two driver units mounted upstream of the injectors at the frequencies of SSO and at four different levels of amplifier voltages (1.5, 2, 2.5, and 3 V) fed to the driver units. Although a representation based on amplifier voltage is not physically relevant, it is provided here as a common ground for SFM between flame image measurement (shown in Fig. 2) and the measurements carried out to obtain the describing functions shown in Fig. 3. Such a representation based on amplifier voltage can alternatively be indicated in terms of relative velocity fluctuations in the chamber $u'_{c,r}/\overline{u}_{c,r}$, as shown in Fig. 3(b).

On comparing the phase of $\mathcal{F}$ at different fluctuation levels (Fig. 3(a) top), it can be seen that there is no discernible nonlinearity with respect to the level of fluctuation, and the phases of $\mathcal{F}$ and $\mathcal{H}$ match quite well. The role of phase on stability analyses (see for example [31, 44]) is critical, and the experimentally observed match validates the usage of FTF/FDF in reduced-order models. Contrary to the phase observation, one may notice the presence of nonlinearity in the gain of SFM (Fig. 3(a) bottom) with respect to the fluctuation level at all the frequencies. Fig. 3(b) shows the gain G_F as a function of velocity fluctuation levels at the four frequencies considered in this study along with G_H. At $f_0 = 448\,\text{Hz}$ and $560\,\text{Hz}$, the fluctuation levels match between SSO and SFM at an amplifier voltage of $2\,\text{V}$ and $2.5\,\text{V}$, respectively, where one may also notice that the gains G_F and G_H match in these two cases. Whereas, at $f_0 = 472\,\text{Hz}$ and $420\,\text{Hz}$ none of the SFM cases matches with the fluctuation level of SSO. Hence, a match of gain between SFM and SSO is not attained, but the respective values are close. These results and the flame images shown in Fig. 2 clearly indicate the importance of utilizing a version of $\mathcal{F}$ that matches with the velocity fluctuation level of $\mathcal{H}$ in the low-order models to have a good prediction of instabilities. If the low-order model uses an $\mathcal{F}$ that does not match the level of SSO, one might still be able to potentially predict whether or not the system will be unstable purely based on the phase information from the FDF. But the prediction of limit cycle amplitude would potentially be erroneous due to the mismatch in gain.

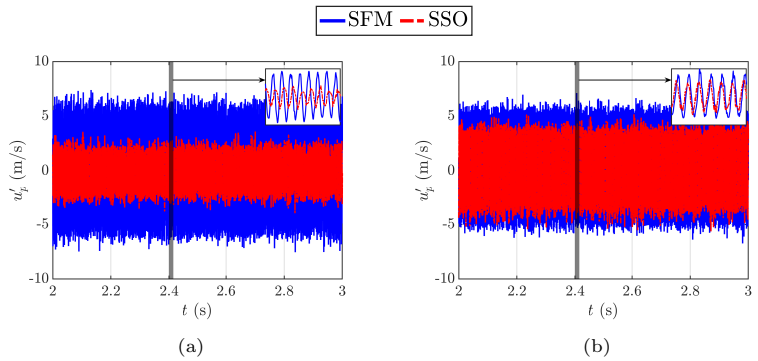

Figure 4: Comparison of time evolution of plenum velocity between an SFM and SSO shown for a period of 1 s. Results are plotted when the chamber velocity fluctuation level of SFM matches with that of SSO. (a) SFM: $V_0 = 2.5\,\text{V}$; SSO: $l_c = 250\,\text{mm}$, $f_0 = 560\,\text{Hz}$ and (b) SFM: $V_0 = 2\,\text{V}$; SSO: $l_c = 315\,\text{mm}$, $f_0 = 448\,\text{Hz}$.

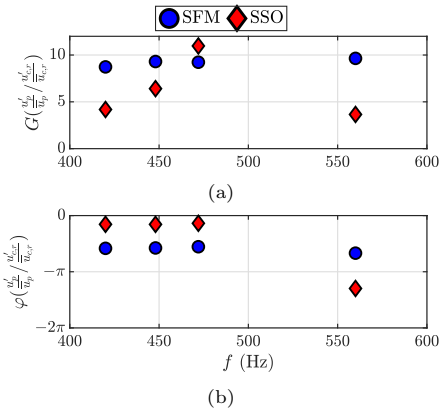

Figure 5: The gain (a) and phase (b) of relative plenum velocity fluctuations to relative chamber velocity fluctuations. At $f_0 = 448\,\text{Hz}$ ($l_c = 315\,\text{mm}$) and $560\,\text{Hz}$ ($l_c = 250\,\text{mm}$), the results are shown when the chamber velocity fluctuations of SFM coincide with those of SSO. At $f_0 = 420\,\text{Hz}$ ($l_c = 350\,\text{mm}$) and $472\,\text{Hz}$ ($l_c = 300\,\text{mm}$), the results are shown when the chamber velocity fluctuations of SFM are closest to SSO.

5. Injector dynamics during SSO and SFM

Although the FTF/FDF framework by definition considers the reference velocity at the base of the flame, it is a common practice to use a velocity reference for the transfer function in the plenum, upstream of the injection unit (this is exemplified in [49], and more recently by [69, 70]). This choice is made because of the practical difficulties associated with the measurement of velocity at the base of the flame, which would mandate some form of an optical measurement technique to access the flame zone. For an acoustically transparent injector that is compact compared to the acoustic wavelength, the velocity upstream and downstream of the injector would remain the same as it stays passive to the acoustic waves. In such a case, the FDF, considering upstream velocity as the reference, would still be valid as the injector dynamics would be the same between SSO, where there is strong pressure oscillation downstream, and during modulation of the flame from upstream. However, the injector considered in the present work is only weakly transparent to acoustic waves due to the high pressure drop and abrupt area changes in the swirler channels. Such injectors act as a loss element by converting some of the incoming acoustic waves into convective waves at the injector outlet. This raises a question on whether the FDF measured with a reference velocity in the plenum and an upstream acoustic modulation would suitably represent the flame dynamics during SSO. Figure 4 shows the time evolution of plenum velocity between SFM and SSO when the chamber velocity $u'_{c,r}$ coincides in two of the investigated cases. The plenum velocity is obtained by the two-microphone method from the pressure signals of the plenum microphones MP1 and MP3 (refer Fig. 1(c)). Chamber velocity is measured by LDA as described in section 2. Figure 4, left shows the plenum velocity during an SSO at $l_c = 250\,\text{mm}$ and SFM at $V_0 = 2.5\,\text{V}$, and on the right is the SSO at $l_c = 315\,\text{mm}$ and SFM at $V_0 = 2\,\text{V}$. It can be seen that for the same level of velocity fluctuations in the chamber, SFM always yields a higher level of plenum velocity u'_p than SSO. This means that the amplitude of the relative velocity fluctuation in the plenum is not preserved between SSO and SFM. Figure 5 shows the gain and phase of relative velocity fluctuations in the plenum to the relative velocity fluctuations in the chamber at different frequencies considered in this study. Here, $\overline{u}_p$ is the bulk velocity in the plenum while $\overline{u}_c$ is the mean velocity at exit of the injector measured at $r = 4\,\text{mm}$ and $h = 2.5\,\text{mm}$. The data plotted at $f_0 = 448\,\text{Hz}$ and $560\,\text{Hz}$ correspond to a situation where the chamber velocity fluctuations nearly coincide for SSO and SFM. At $f_0 = 420\,\text{Hz}$ and $472\,\text{Hz}$, the data points pertain to a situation where the velocity fluctuations in the chamber of SFM are closest to the SSO case but do not quite match. Significant differences can be observed between SSO and SFM with regard to the velocity fluctuation ratio, with the gain during SFM being twice as high as that corresponding to SSO for most frequencies, except at $472\,\text{Hz}$, where this difference is minor. It is also found that under SFM, the phase between plenum and chamber velocity fluctuations remains the same at all frequencies and is slightly higher than $-\pi/2$. However, when the system is under SSO, the phase is rather close to 0 at lower frequencies and close to $-\pi$ at $560\,\text{Hz}$. Differences in the dynamical state of a swirling injector system submitted to upstream and downstream modulation observed in [71] are analogous to those found in the present investigation if one considers that the downstream modulation state is similar to SSO, where pressure oscillations originate from downstream combustion processes. A velocity measurement performed upstream of the injector would, in fact, lump the injector and flame dynamics together and will not suitably represent the flame dynamics under SSO. Thus, for an injector that is weakly-transparent to acoustic waves, the velocity measurement for FDF determination should be positioned at the injector outlet. Alternatively, one might consider measuring the injector transfer function under cold flow conditions and extracting it from the lumped injector and flame transfer function, in a way similar to that used in the FTM framework [63]. There are, however, differences in the injector transfer function gain with and without flame (not shown here), thus emphasizing the need for directly obtaining the flame transfer/describing function. This direct determination requires that the incident fluctuations be measured at a point where the relative velocity fluctuations coincide with the relative volumetric fluctuations to be suitably used in the FDF framework as proposed in [65]. It was suggested by a reviewer that the behavior described in this section might be represented by the injector transfer matrix model described in [23, 72] and designated as the $L - \zeta$ model. In this model, the injector transfer matrix $\boldsymbol{B}$ features elements $B_{21} = 0$ and $B_{22} = 1$ [72] or $B_{22} = A_u/A_d$ (where A_u and A_d are the upstream and downstream cross sectional areas) [23]. A rapid inspection indicates that this might not account for the large drop in fluctuation level and shift in phase observed between the upstream and downstream velocity

fluctuation levels under SFM.

6. Conclusions

Although many theoretical models in combustion instability rely on transfer functions or describing functions, it was essential to see if these concepts are effectively applicable, and in particular, if they can be used in the case of complex multidimensional turbulent spray flames formed by swirling injectors. This central question is investigated by comparing two situations: the first corresponding to a well-established limit cycle self-sustained oscillation (SSO), while the second may be assimilated to an stable flame modulation (SFM) in which the acoustic coupling is minimized, and the flame is externally modulated. Three levels of external modulation are chosen—same, lower, and higher levels than the SSO fluctuations. It is shown that the flame dynamics observed using Abel-transformed OH^* light intensity images matches best when the levels of acoustic oscillation in the two situations are equal. It is also found that the gain of the flame describing function (FDF) is close to that of the flame response measured under SSO when the level of oscillation in the externally modulated flame (SFM case) equals that found under SSO. The level of fluctuation does not affect the phase, and all the SFM cases match the SSO tests. These elements confirm that the FDF framework is applicable and that it is crucial to consider the dependence of flame response on the level of incident perturbations. Additionally, it is shown that the injector dynamics during SFM and SSO are not the same for the case of an injector that is weakly-transparent to acoustic waves. It is advisable to calculate the FDF with respect to relative velocity fluctuations in the chamber since the use of plenum velocity would lump the dynamics of injector and flame together and may fail to represent the flame dynamics under SSO in the absence of a suitable description of the injector's frequency response. The FDF obtained with plenum velocity would neither have the correct gain nor the correct phase evolution, and it will not be possible to predict the unstable operating points with the corresponding low-order model. The present experiments, although restricted to a specific case, provide a direct validation of the FDF concept in the analysis of combustion instabilities leading to limit cycle oscillations.

Acknowledgments

This article is dedicated to the memory of Shôn Ffowcs Williams. One of the authors (S. Candel) had the privilege to meet Shôn at an early stage. After a seminar in Cambridge, Shôn drove him on small British country roads from Cambridge to Bristol to participate to the "Noise panel" while discussing aeroacoustics, noise from entropy spots traveling through nozzles and turbines, and many other issues. S. Candel has kept vibrant memories of this initial encounter with an admirable scientist. The authors wish to thank the reviewers for their helpful comments. The present work benefited from the support of project FASMIC ANR16-CE22-0013 of the French National Research Agency (ANR) and of the European Union's Horizon 2020 research and innovation programme, Annulight with grant agreement no. 765998.

Appendix A. A model problem featuring self-sustained oscillations and allowing stable flame modulation

We consider, in this appendix, a model problem in which a flame placed in a duct may become unstable and leads to an oscillation, and in which it is also possible to apply an external modulation to determine the flame describing function (FDF). This appendix is intended to respond to one of the reviewer's comments. The objective is to show in an idealized case what distinguishes the situation where the flame executes a self-sustained oscillation (SSO) from that where the system is stable and modulated externally to determine the FDF (referred to as stable flame modulation or SFM). The geometry of the problem shown in Fig. A.6 features a driver unit on the left that may be passive i.e. $u'_f = 0$, or may impose a velocity perturbation $u'_f = v_0 e^{-i\omega t}$. The flame is located at a distance a from the upstream end of the duct. The downstream end is open, and its length l already includes the so-called "end correction", so that one may write $p'(l) = 0$. Regions 1 and 2 respectively correspond to upstream $0 \leq x \leq a$ and to downstream $b \leq x \leq l$ of the flame.

For simplicity, one assumes that the temperatures on the two sides of the flame are the same so that the densities, sound velocities, and wave numbers are the same in the two regions. The jump conditions at the flame expresses pressure continuity such that $p'_1(x=a) = p'_2(x=a)$, and the acoustic volume flow rate is defined by the heat release rate fluctuation of the flame:

$$Su'_2 - Su'_1 = \frac{\gamma - 1}{\rho_0 c^2}\dot{Q}' \tag{A.1}$$

It is possible to express the heat release rate in the flame by making use of the flame describing function $\mathcal{F}$. One obtains after standard calculations,

$$u'_2 - u'_1 = \widehat{\mathcal{F}} u'_1 \tag{A.2}$$

where $\widehat{\mathcal{F}} = \Theta\mathcal{F}$ with $\Theta = (T_2/T_1) - 1$. With a set of standard calculations, one may obtain the various field constants $A...D$ and express the velocity disturbance on the upstream side of the flame in the form:

$$u'_1(x=a) = \frac{v_0}{\mathcal{D}(\omega)}[\mathrm{i}\mathrm{e}^{-\mathrm{i}kl}\sin ka + \mathrm{e}^{-\mathrm{i}ka}\cos kl] \tag{A.3}$$

where $\mathcal{D}(\omega) = \cos kl - \widehat{\mathcal{F}}\sin ka \sin kb$ designates the dispersion relation of the system. It is then easy to

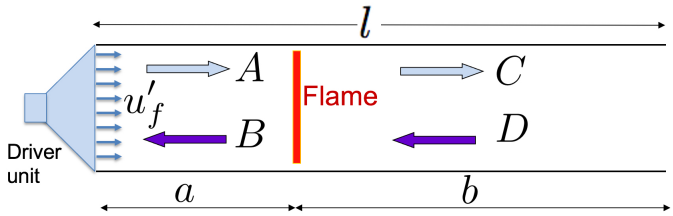

Figure A.6: Model problem. The combustion system comprises a driver unit on the upstream side, an open end downstream. A compact flame is located at a distance $x = a$ from the inlet. The driver unit modulates the flame with a velocity $u'_f = v_0\mathrm{e}^{-\mathrm{i}\omega t}$.

deduce the heat release rate fluctuation induced by this velocity fluctuation as,

$$\dot{Q}' = \overline{\dot{Q}}\mathcal{F}\frac{u'_1}{\overline{u}} = \overline{\dot{Q}}\mathcal{F}(\omega, u')\frac{v_0}{\overline{u}}\frac{1}{\mathcal{D}(\omega)}[\mathrm{i}\mathrm{e}^{-\mathrm{i}kl}\sin ka + \mathrm{e}^{-\mathrm{i}ka}\cos kl] \tag{A.4}$$

These expressions give rise to two different situations. In the first, designated in this article as SSO, the dispersion relation $\mathcal{D}(\omega) = 0$ has complex roots, and one of these roots has a positive imaginary part. This may give rise to unstable oscillations that will eventually lead to a limit cycle because of nonlinear mechanisms represented by the describing function. The second possibility is to avoid having an oscillatory operating regime by moving the complex roots of the dispersion relation and shifting them in the high frequency range where the describing function features low gain values. We know that combustion oscillations generally occur at a frequency corresponding to one of the natural resonant modes of the system. These eigenfrequencies are given by the dispersion relation in the absence of a flame, i.e., $\cos kl = 0$. The first of these eigenfrequencies corresponds to the 1L (quarter wave) mode and is given by $\omega_0^1 = (\pi/2)(c/l)$. If l is made sufficiently short, this eigenfrequency takes large values, and one may expect that the FDF gain corresponding to this eigenfrequency will be small: $|\widehat{\mathcal{F}}(\omega_0^1)| << 1$. For the range of angular frequencies that is well below ω_0^1, ka will take small values $ka << 1$, since a is a fraction of l. One then finds that $\mathcal{D}(\omega) \simeq \cos kl$. The velocity fluctuation on the upstream side of the flame given by expression (A.3) then becomes:

$$u'_1(x=a) \simeq \frac{v_0}{\mathcal{D}(\omega)}(\cos kl) \tag{A.5}$$

Using the approximate expression of $\mathcal{D}(\omega)$, one arrives at the result that $u'_1(x=a) \simeq v_0$. The velocity fluctuation on the upstream side of the flame is nearly identical to the velocity modulation imposed on the system u'_f. In essence, the flame has been stabilized by reducing the feedback contribution to the velocity

disturbance that is incident to the flame. The feedback is present, but its contribution has been made negligible. One may then measure $u_1'(x=a)$, determine $\dot{Q}'$, and deduce $\mathcal{F}$ from these measurements. This second situation is designated in this article as SFM. It clearly allows the determination of the FDF using harmonic forcing.

References

[1] J. E. Ffowcs Williams, Review lecture - Anti-sound, Proc. R. Soc. A: Math. Phys. Eng. Sci. 395 (1984) 63–88. doi:doi.org/10.1098/rspa.1984.0090.

[2] J. E. Ffowcs Williams, M. F. L. Harper, D. J. Allwright, Active stabilization of compressor instability and surge in a working engine, J. Turbomach. 115 (1993) 68–75. doi:doi.org/10.1115/1.2929219.

[3] J. E. Ffowcs Williams, Active flow control, J. Sound Vib. 239 (2001) 861–871. doi:doi.org/10.1006/jsvi.2000.3225.

[4] J. E. Ffowcs Williams, Noise, anti-noise and fluid flow control, Philos. Trans. R. Soc. A: Math. Phys. Eng. Sci. 360 (2002) 821–832. doi:doi.org/10.1098/rsta.2001.0969.

[5] D. G. Crighton, A. P. Dowling, J. E. Ffowcs Williams, M. Heckl, F. G. Leppington, Modern methods in analytical acoustics (Chapter 13. Thermoacoustic sources and instabilities) pp 378-405, Springer, London, 1992. doi:doi.org/10.1007/978-1-4471-0399-8.

[6] A. P. Dowling, S. R. Stow, Acoustic analysis of gas turbine combustors, J. Propuls. Power 19 (2003) 751–764. doi:doi.org/10.2514/2.6192.

[7] K. R. McManus, T. Poinsot, S. Candel, A review of active control of combustion instabilities, Prog. Energy Combust. Sci. 19 (1993) 1–29. doi:doi.org/10.1016/0360-1285(93)90020-F.

[8] A. M. Annaswamy, M. Fleifil, J. P. Hathout, A. F. Ghoniem, Impact of linear coupling on the design of active controllers for the thermoacoustic instability, Combust. Sci. Technol. 128 (1997) 131–180. doi:doi.org/10.1080/00102209708935707.

[9] S. Candel, Combustion dynamics and control: progress and challenges, Proc. Combust. Inst. 29 (2002) 1–28. doi:doi.org/10.1016/S1540-7489(02)80007-4.

[10] A. P. Dowling, A. S. Morgans, Feedback control of combustion oscillations, Annu. Rev. Fluid Mech. 37 (2005) 151–182. doi:doi.org/10.1146/annurev.fluid.36.050802.122038.

[11] A. S. Morgans, S. R. Stow, Model-based control of combustion instabilities in annular combustors, Combust. Flame 150 (4) (2007) 380–399. doi:doi.org/10.1016/j.combustflame.2007.06.002.

[12] L. Crocco, Aspects of combustion stability in liquid propellant rocket motors. Part I., J. Am. Rocket Soc. 21 (1951) 163–178. doi:doi.org/10.2514/8.4393.

[13] L. Crocco, Aspects of combustion stability in liquid propellant rocket motors. Part II., J. Am. Rocket Soc. 22 (1952) 7–16. doi:doi.org/10.2514/8.4410.

[14] H. S. Tsien, Servo-stabilization of combustion in rocket engines, J. Am. Rocket Soc. 22 (256–263) (1952). doi:doi.org/10.2514/8.4488.

[15] F. E. Marble, D. W. Cox Jr, Servo-stabilization of low frequency oscillations in a liquid bipropellant rocket motor, J. Am. Rocket Soc. 23 (63–74) (1953). doi:doi.org/10.2514/8.4542.

[16] L. Crocco, S. Cheng, Theory of combustion instability in liquid propellant rocket motors, Butterworths Scientific Publications, New York, 1956.

[17] D. J. Harrje, F. H. Reardon, Liquid propellant rocket instability, Tech. rep., NASA, Report SP-194 (1972).

[18] V. Yang, W. Anderson, Liquid Rocket Engine Combustion Instability, Am. Inst. Aeronaut. Astronaut., 1995.

[19] G. A. Richards, M. C. Janus, Characterization of oscillations during premix gas turbine combustion, J. Eng. Gas Turb. Power 120 (1998) 294–302. doi:doi.org/10.1115/1.2818120.

[20] T. Lieuwen, B. T. Zinn, The role of equivalence ratio oscillations in driving combustion instabilities in low NOx gas turbines, Proc. Combust. Inst. 27 (1998) 1809–1816. doi:doi.org/10.1016/S0082-0784(98)80022-2.

[21] T. Lieuwen, H. Torres, C. Johnson, B. T. Zinn, A mechanism of combustion instability in lean premixed gas turbine combustors, J. Eng. Gas Turb. Power 123 (2001) 182–189. doi:doi.org/10.1115/1.1339002.

[22] S. Hubbard, A. P. Dowling, Acoustic resonances of an industrial gas turbine combustion system, J. Eng. Gas Turb. Power 123 (2001) 766–773. doi:doi.org/10.1115/1.1370975.

[23] C. O. Paschereit, B. Schuermans, W. Polifke, O. Mattson, Measurement of transfer matrices and source terms of premixed flames, J. Eng. Gas Turb. Power 124 (2) (2002) 239–247. doi:https://doi.org/10.1115/1.1383255.

[24] T. C. Lieuwen, V. Yang, Combustion instabilities in gas turbines, Operational experience, Fundamental mechanisms, and Modeling, Prog. Astronaut. Aeronaut., Am. Inst. Aeronaut. Astronaut., Inc., 2005.

[25] K.-U. Schildmacher, R. Koch, H.-J. Bauer, Experimental characterization of premixed flame instabilities of a model gas turbine burner, Flow Turbul. Combust. 76 (2006) 177–197. doi:doi.org/10.1007/s10494-006-9012-z.

[26] Y. Huang, V. Yang, Dynamics and stability of lean-premixed swirl-stabilized combustion, Prog. Energy Combust. Sci. 35 (2009) 293–384. doi:doi.org/10.1016/j.pecs.2009.01.002.

[27] W. Krebs, H. Krediet, E. Portillo, S. Hermeth, T. Poinsot, S. Schimek, C. O. Paschereit, Comparison of nonlinear to linear thermoacoustic stability analysis of a gas turbine combustion system, J. Eng. Gas Turb. Power 135 (2013) 081503. doi:doi.org/10.1115/1.4023887.

[28] S. Candel, D. Durox, T. Schuller, J.-F. Bourgouin, J. P. Moeck, Dynamics of swirling flames, Annu. Rev. Fluid Mech. 46 (2014) 147–173. doi:doi.org/10.1146/annurev-fluid-010313-141300.

[29] T. Poinsot, Prediction and control of combustion instabilities in real engines, Proc. Combust. Inst. 36 (2017) 1–28. doi:doi.org/10.1016/j.proci.2016.05.007.

[30] W. Polifke, Modeling and analysis of premixed flame dynamics by means of distributed time delays, Prog. Energy Combust. Sci. 79 (2020) 100845. doi:doi.org/10.1016/j.pecs.2020.100845.
[31] T. Schuller, T. Poinsot, S. Candel, Dynamics and control of premixed combustion systems based on flame transfer and describing functions, J. Fluid Mech. 894 (2020) 1–95. doi:doi.org/10.1017/jfm.2020.239.
[32] Y. Matsui, An experimental study on pyro-acoustic amplification of premixed laminar flames, Combust. Flame 43 (1981) 199–209. doi:doi.org/10.1016/0010-2180(81)90017-1.
[33] M. Fleifil, A. M. Annaswamy, Z. A. Ghoneim, A. F. Ghoniem, Response of a laminar premixed flame to flow oscillations: A kinematic model and thermoacoustic instability results, Combust. Flame 106 (1996) 487–510. doi:doi.org/10.1016/0010-2180(96)00049-1.
[34] S. Ducruix, D. Durox, S. Candel, Theoretical and experimental determinations of the transfer function of a laminar premixed flame, Proc. Combust. Inst. 28 (2000) 765–773. doi:doi.org/10.1016/S0082-0784(00)80279-9.
[35] T. Schuller, S. Ducruix, D. Durox, S. Candel, Modeling tools for the prediction of premixed Flame Transfer Functions, Proc. Combust. Inst. 29 (2002) 107–113. doi:doi.org/10.1016/S1540-7489(02)80018-9.
[36] T. Schuller, D. Durox, S. Candel, A unified model for the prediction of laminar flame transfer functions : comparisons between conical and V-flame dynamics, Combust. Flame 134 (2003) 21–34. doi:doi.org/10.1016/S0010-2180(03)00042-7.
[37] T. Lieuwen, Modeling premixed combustion-acoustic wave interactions: A review, J. Propuls. Power 19 (2003) 765–779. doi:doi.org/10.2514/2.6193.
[38] Preetham, T. Sai Kumar, T. Lieuwen, Response of premixed flames to flow oscillations : unsteady curvature effects, 44th AIAA Aerosp. Sci. Meet. Exhib. Paper 2006-960 (2006). doi:doi.org/10.2514/6.2006-960.
[39] Preetham, H. Santosh, T. Lieuwen, Dynamics of laminar premixed flames forced by harmonic velocity disturbances, J. Propuls. Power 24 (2008) 1390–1402. doi:doi.org/10.2514/1.35432.
[40] P. Palies, T. Schuller, D. Durox, S. Candel, Modeling of swirling flames transfer functions, Proc. Combust. Inst. 33 (2011) 2967–2974. doi:doi.org/10.1016/j.proci.2010.06.059.
[41] K. T. Kim, D. A. Santavicca, Generalization of turbulent swirl flame transfer functions in gas turbine combustors, Combust. Sci. Tech. 185 (2013) 999–1015. doi:doi.org/10.1080/00102202.2012.752734.
[42] V. N. Kornilov, M. Manohar, L. P. H. de Goey, Thermo-acoustic behavior of multiple flame burner decks: transfer function decomposition, Proc. Combust. Inst. 32 (2009) 1383–1390. doi:doi.org/10.1016/j.proci.2008.05.022.
[43] A. P. Dowling, Nonlinear self-excited oscillations of a ducted flame, J. Fluid Mech. 346 (1997) 271–290. doi:doi.org/10.1017/S0022112097006484.
[44] N. Noiray, D. Durox, T. Schuller, S. Candel, A unified framework for nonlinear combustion instability analysis based on the flame describing function, J. Fluid Mech. 615 (2008) 139–167. doi:doi.org/10.1017/S0022112008003613.
[45] D. Durox, T. Schuller, N. Noiray, S. Candel, Experimental analysis of nonlinear flame transfer functions for different flame geometries, Proc. Combust. Inst. 32 (2009) 1391–1398. doi:doi.org/10.1016/j.proci.2008.06.204.
[46] N. Noiray, D. Durox, T. Schuller, S. Candel, A method for estimating the noise level of unstable combustion based on the flame describing function, Int. J. Aeroacoust. 8 (2009) 157–176. doi:doi.org/10.1260/147547209786234957.
[47] F. Boudy, D. Durox, T. Schuller, S. Candel, Nonlinear mode triggering in a multiple flame combustor, Proc. Combust. Inst. 33 (2011) 1121–1128. doi:doi.org/10.1016/j.proci.2010.05.079.
[48] F. Boudy, D. Durox, T. Schuller, G. Jomaas, S. Candel, Describing function analysis of limit cycles in a multiple flame combustor, J. Eng. Gas Turb. Power 133 (2011) 061502. doi:doi.org/10.1115/1.4002275.
[49] P. Palies, D. Durox, T. Schuller, S. Candel, Nonlinear combustion instability analysis based on the flame describing function applied to turbulent premixed swirling flames, Combust. Flame 158 (2011) 1980–1991. doi:doi.org/10.1016/j.combustflame.2011.02.012.
[50] M. A. Heckl, Analytical model of nonlinear thermo-acoustic effects in a matrix burner, J. Sound Vib. 332 (2013) 4021–4036. doi:doi.org/10.1016/j.jsv.2012.11.010.
[51] C. F. Silva, F. Nicoud, T. Schuller, D. Durox, S. Candel, Combining a Helmholtz solver with the flame describing function to assess combustion instability in a premixed swirled combustor, Combust. Flame 160 (2013) 1743–1754. doi:doi.org/10.1016/j.combustflame.2013.03.020.
[52] X. Han, A. S. Morgans, Simulation of the flame describing function of a turbulent premixed flame using an open-source LES solver, Combust. Flame 162 (2015) 1778–1792. doi:doi.org/10.1016/j.combustflame.2014.11.039.
[53] X. Han, J. Li, A. S. Morgans, Prediction of combustion instability limit cycle oscillations by combining flame describing function simulations with a thermoacoustic network model, Combust. Flame 162 (2015) 3632–3647. doi:doi.org/10.1016/j.combustflame.2015.06.020.
[54] M. Heckl, A new perspective on the flame describing function of a matrix flame, Int. J. Spray Combust. Dyn. 7 (2015) 91–112. doi:doi.org/10.1260/1756-8277.7.2.91.
[55] S. M. Gopinathan, D. Iurashev, A. Bigongiari, M. Heckl, Nonlinear analytical flame models with amplitude-dependent time-lag distributions, Int. J. Spray Combust. Dyn. 10 (2018) 264–276. doi:doi.org/10.1177/1756827717728056.
[56] G. Ghirardo, M. P. Juniper, J. P. Moeck, Weakly nonlinear analysis of thermoacoustic instabilities in annular combustors, J. Fluid Mech. 805 (2016) 52–87. doi:doi.org/10.1017/jfm.2016.494.
[57] D. Laera, T. Schuller, K. Prieur, D. Durox, S. M. Camporeale, S. Candel, Flame describing function analysis of spinning and standing modes in an annular combustor and comparison with experiments, Combust. Flame 184 (2017) 136–152. doi:doi.org/10.1016/j.combustflame.2017.05.021.
[58] M. Haeringer, M. Merk, W. Polifke, Inclusion of higher harmonics in the flame describing function for predicting limit cycles of self-excited combustion instabilities, Proc. Combust. Inst. 37 (2019) 5255–5262. doi:doi.org/10.1016/j.proci.2018.06.150.
[59] P. Rajendram Soundararajan, G. Vignat, D. Durox, A. Renaud, S. Candel, Effect of different fuels on combustion instabilities in an annular combustor, J. Eng. Gas Turb. Power 143 (2021) 031007. doi:doi.org/10.1115/1.4049702.

[60] J. P. Moeck, C. O. Paschereit, Nonlinear interactions of multiple linearly unstable thermoacoustic modes, Int. J. Spray Combust. Dyn. 4 (2012) 1–27. doi:doi.org/10.1260/1756-8277.4.1.1.
[61] A. Orchini, M. P. Juniper, Flame double input describing function analysis, Combust. Flame 171 (2016) 87–102. doi:doi.org/10.1016/j.combustflame.2016.06.014.
[62] I. R. Hurle, R. B. Price, T. M. Sugden, A. Thomas, Sound emission from open turbulent premixed flames, Proc. R. Soc. A: Math. Phys. Eng. Sci. 303 (1968) 409–427. doi:doi.org/10.1098/rspa.1968.0058.
[63] B. Schuermans, V. Bellucci, F. Guethe, F. Meili, P. Flohr, C. O. Paschereit, A detailed analysis of thermoacoustic interaction mechanisms in a turbulent premixed flame, in: Turbo Expo: Power for Land, Sea, and Air paper no. GT2004-53831, Vol. 1, 2004, pp. 539–551. doi:doi.org/10.1115/GT2004-53831.
[64] N. Noiray, D. Durox, T. Schuller, S. Candel, Mode conversion in acoustically modulated confined jets, Am. Inst. Aeronaut. Astronaut. J. 47 (2009) 2053–2062. doi:doi.org/10.2514/1.37734.
[65] P. Rajendram Soundararajan, D. Durox, A. Renaud, G. Vignat, S. Candel, Swirler effects on combustion instabilities analyzed with measured FDFs, injector impedances and damping rates, Combust. Flame 238 (2022) 111947. doi:doi.org/10.1016/j.combustflame.2021.111947.
[66] G. Vignat, P. Rajendram Soundararajan, D. Durox, A. Vié, A. Renaud, S. Candel, A joint experimental and large eddy simulation characterization of the liquid fuel spray in a swirl injector, J. Eng. Gas Turb. Power 143 (2021) 081019. doi:doi.org/10.1115/1.4049771.
[67] A. F. Seybert, D. F. Ross, Experimental determination of acoustic properties using a two-microphone random-excitation technique, J. Acous. Soc. Am. 61 (1977) 1362–1370. doi:doi.org/10.1121/1.381403.
[68] A. Degenève, R. Vicquelin, C. Mirat, B. Labegorre, P. Jourdaine, J. Caudal, T. Schuller, Scaling relations for the length of coaxial oxy-flames with and without swirl, Proc. Combust. Inst. 37 (2019) 4563–4570. doi:doi.org/10.1016/j.proci.2018.06.032.
[69] M. Gatti, R. Gaudron, C. Mirat, L. Zimmer, T. Schuller, Impact of swirl and bluff-body on the transfer function of premixed flames, Proc. Combust. Inst. 37 (2019) 5197–5204. doi:doi.org/10.1016/j.proci.2018.06.148.
[70] G. Wang, T. F. Guiberti, X. Xia, L. Li, X. Liu, W. L. Roberts, F. Qi, Decomposition of swirling flame transfer function in the complex space, Combust. Flame 228 (2021) 29–41. doi:doi.org/10.1016/j.combustflame.2021.01.032.
[71] R. Gaudron, M. Gatti, C. Mirat, T. Schuller, Flame describing functions of a confined premixed swirled combustor with upstream and downstream forcing, J. Eng. Gas Turb. Power 141 (2019) 051016. doi:doi.org/10.1115/1.4041000.
[72] V. Bellucci, B. Schuermans, D. Nowak, P. Flohr, C. O. Paschereit, Thermoacoustic modeling of a gas turbine combustor equipped with acoustic dampers, J. Turbomach. 127 (2005) 372–379. doi:doi.org/10.1115/1.1791284.